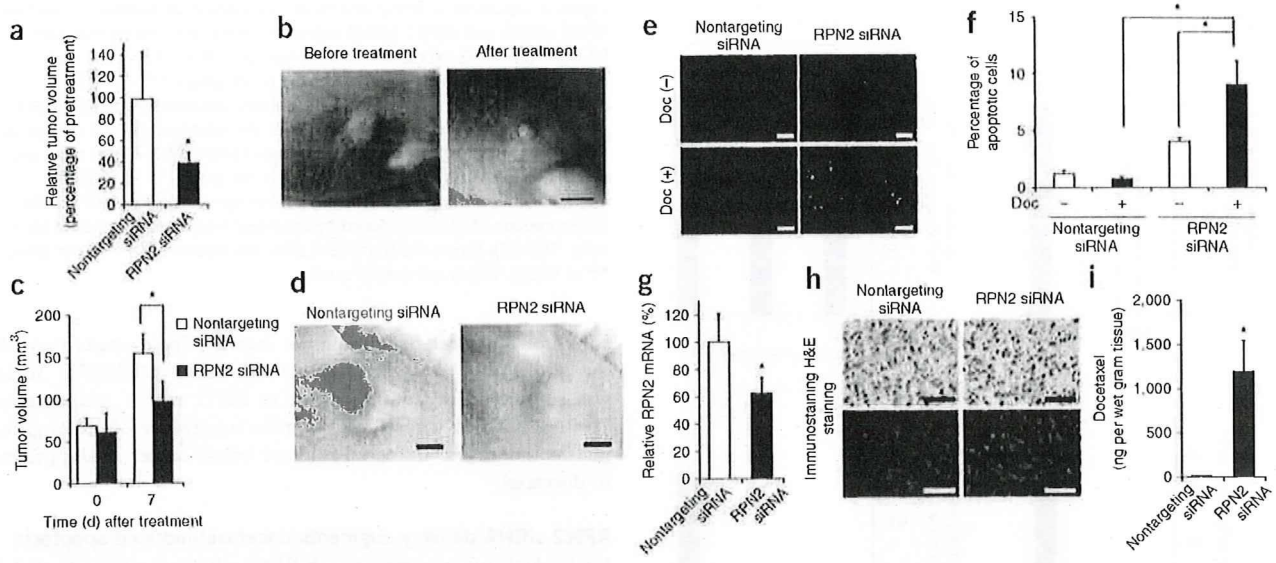

Figure 4 Delivery of RPN2 siRNA to docetaxel-resistant breast tumors. The effect of RPN2 siRNA was examined in orthotopic breast tumor models. **(a)** Reduction of MCF7-ADR breast tumor volume in mice given RPN2 siRNA or control nontargeting siRNA along with docetaxel ($n = 6$ per group, $^*P < 0.01$). **(b)** siRNA-treated MCF7-ADR tumors in mice before and 7 d after docetaxel treatment. Scale bar, 5 mm. **(c)** Growth of MDA-MB-231/MDR1 breast tumor in mice administered RPN2 siRNA or nontargeting siRNA along with docetaxel ($n = 6$ per group, $^*P < 0.002$). **(d)** MDA-MB-231/MDR1 tumors in mice 7 d after treatment with siRNA and docetaxel. Scale bar, 5 mm. **(e)** TUNEL staining of MCF7-ADR tumor tissues treated with RPN2 siRNAs or nontargeting siRNAs in the presence or absence of docetaxel. Scale bar, 50 μm. **(f)** TUNEL-positive cells were counted and are represented in the graph ($n = 3$ per group, $^*P < 0.01$). **(g)** Expression of RPN2 mRNA in MCF7-ADR tumors treated with RPN2 siRNAs or nontargeting siRNAs ($n = 3$ per group, $^*P < 0.01$). **(h)** Expression of RPN2 protein in MCF7-ADR tumors. H&E staining and RPN2 immunofluorescence staining (green, RPN2; blue, nuclei) of tissues treated with RPN2 siRNA or nontargeting siRNA. Scale bar, 50 μm. **(i)** Docetaxel retention in MCF7-ADR tumors in mice treated with RPN2 siRNAs or nontargeting siRNAs ($n = 4$ per group, $^*P < 0.001$). Values are means ± s.d.

in MCF7-ADR cells transduced by RPN2 siRNA (**Supplementary Fig. 4** online). For this reason, and to assess the potential involvement of *RPN2* gene overexpression in MDR1 functions, we tested the glycosylation status of MDR1 protein in MCF7-ADR cells transfected with RPN2 siRNA. We analyzed the glycosylation patterns by western blotting of P-glycoprotein, which appears on blots as mature 170-kDa, immature (partially glycosylated) 150-kDa and unglycosylated 140-kDa bands[28]. The 150-kDa immature and 140-kDa unglycosylated P-glycoproteins were clearly found in MCF7-ADR cells with RPN2 knockdown (90% inhibition of mRNA by real-time RT-PCR analysis; **Fig. 5a**). More than 80% of P-glycoproteins were unglycosylated or partially glycosylated in RPN2-silenced cells (composition of P-glycoproteins, 170 kDa:150 kDa:140 kDa = 18:40:42). In contrast, MCF7-ADR cells transduced with nontargeting control siRNA expressed more than half of their P-glycoproteins as170-kDa mature P-glycoprotein (170 kDa:150 kDa:140 kDa = 52:17:31). This result showed that RPN2 knockdown inhibits glycosylation of P-glycoproteins in MCF7-ADR cells. The western blot of P-glycoprotein, particularly in cells transduced with RPN2 siRNA, showed 'smear' patterns (**Fig. 5a**). We speculated that the smear pattern was caused by the presence of intermediately glycosylated forms in various sizes. We treated the cell lysate samples with peptide:*N*-glycosidase F (PNGase F) to remove *N*-glycan chains, which shifted the P-glycoprotein in the blot from a smear pattern to a 140-kDa unglycosylated protein band in MCF7-ADR cell lysates. After PNGase F treatment, both nontargeting control siRNA– and RPN2 siRNA–transduced cells showed a 140-kDa unglycosylated P-glycoprotein band (**Fig. 5a**). This indicates that the smear pattern resulted from the presence of intermediately glycosylated P-glycoprotein and that there were a number of intermediately glycosylated P-glycoproteins in the RPN2-silenced cells because of inhibition of glycosylation on P-glycoprotein.

We further evaluated the RPN2 siRNA effects on cell surface P-glycoprotein expression in MCF7-ADR cells by immunofluorescence staining. As expected, immunofluorescence staining indicated that P-glycoprotein was predominantly localized to the cell membrane in MCF7-ADR cells transduced with control nontargeting siRNAs, whereas the intensity of membrane P-glycoprotein in RPN2-downregulated cells was considerably reduced (**Fig. 5b**). Moreover, retention of rhodamine-123, which is a substrate of P-glycoprotein, was strongly enhanced in MCF7-ADR cells transfected with RPN2 siRNA compared to those transfected with nontargeting siRNA (**Fig. 5c**). This indicates that downregulation of RPN2 restores drug retention and inhibits P-glycoprotein function by suppressing the glycosylation of P-glycoproteins in MCF7-ADR cells.

To further bolster these findings, we performed immunostaining analysis of RPN2 and P-glycoprotein in MCF7-ADR tumors in mice. The RPN2 shutdown resulted in a marked disappearance of the membrane-bound P-glycoprotein (**Fig. 5d**), an observation that supports our *in vitro* findings that RPN2 downregulation by siRNA in drug-resistant MCF7-ADR cells results in the loss of membrane-bound P-glycoprotein.

Furthermore, we have examined the status of RPN2 and P-glycoprotein in breast cancer tissues from subjects with RPN2 mRNA high expression ($n = 4$) and RPN2 mRNA low expression ($n = 4$) by immunostaining. P-glycoprotein was predominantly localized to the cell membrane in the primary tumor with a strong signal for RPN2, whereas in the primary tumor with low expression of RPN2, P-glycoprotein was found in the cytoplasm (**Supplementary**

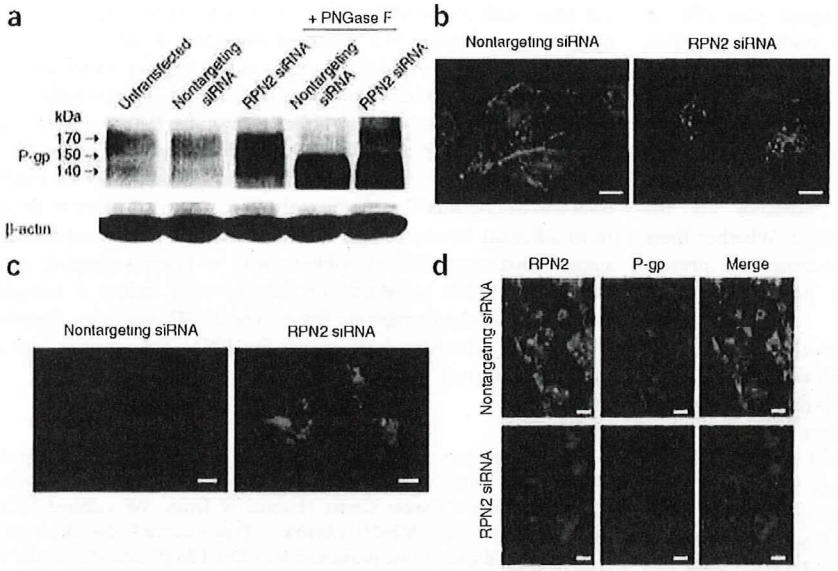

Figure 5 RPN2 siRNA regulates glycosylation of P-glycoprotein (P-gp). **(a)** Western blot analysis shows the glycosylation status of P-gp in MCF7-ADR cells 72 h after transfection of RPN2 siRNA or control nontargeting siRNA. Bands migrating at 170, 150 and 140 kDa represent mature, immature and unglycosylated forms of P-gp, respectively. **(b)** Immunofluorescence staining of P-gp on MCF7-ADR cell membrane surfaces. Cells were treated with RPN2 siRNA or nontargeting siRNA for 72 h. Scale bar, 5 μm. **(c)** Rhodamine-123 retention in MCF7-ADR cells 72 h after transfection with RPN2 siRNA or control nontargeting siRNA. Scale bar, 5 μm. **(d)** Localization of P-gp in tumors of MCF7-ADR in mice. Immunofluorescence staining of RPN2 (green) and P-gp (red) are shown. Nuclei are blue (DAPI). Merged images are also shown. Scale bar, 5 μm.

Fig. 5a,b online). Similar results were observed for other breast cancer tissues (**Supplementary Fig. 5c**).

Thus, these data provide a clear link between the glycosylation status of P-glycoprotein and RPN2 expression in drug-resistant breast cancer cells, and the disappearance of the membrane-bound P-glycoprotein leads to a reversal of the multidrug- resistant phenotype.

DISCUSSION

Cancer researchers today are confronted with how to best identify and select the next generation of molecular targets for oncology. An impressive array of potential new cellular targets, suitable for therapeutic intervention, has been revealed by the recent completion of the human genome sequencing project. Approaches as varied as transcription profiling, proteomics and the use of siRNAs are all being exploited in the race to select the most promising candidate drug targets. We tested the feasibility of using atelocollagen-mediated RNAi delivery *in vitro* and *in vivo* to obtain an unbiased evaluation on the efficacy of a specific siRNA related to drug resistance in human breast cancer. We show here that, among genes whose expression was elevated in nonresponders to docetaxel, the siRNA designed for *RPN2* significantly promoted docetaxel-dependent apoptosis and cell growth inhibition of MCF7-ADR human breast cancer cells that exhibit docetaxel resistance. A clinicopathological study showed that there is a significant association of *RPN2* expression with a pathologic response to docetaxel. Most notably, atelocollagen-mediated *in vivo* delivery of RPN2 siRNA significantly reduced the size of orthotopic MCF7-ADR tumors in mice given docetaxel.

In this study, we demonstrated that the atelocollagen delivery system markedly enhanced the efficiency of siRNA for the inhibition of RPN2 in mouse tumor models of human breast cancer. Because siRNA shows very low efficiency in gene silencing *in vivo*, various delivery methods, such as the use of plasmids and viral vectors encoding siRNA and the use of lipids, have been investigated. We have previously shown that the atelocollagen-mediated systemic delivery of siRNA might be a unique strategy for the inhibition of bone-metastatic prostate tumor growth[22]. The siRNA-atelocollagen complex is a nano-sized particle and is stable *in vitro* and *in vivo*[21,29]. Furthermore, we have previously confirmed that the atelocollagen complex shows low toxicity and low immunogenicity *in vivo*[23,24]. Thus, an atelocollagen-mediated local or systemic delivery system holds great potential for the practical application of gene suppression using siRNAs for cancer therapeutics.

Targeting of P-glycoprotein by small-molecular compounds, antibodies or both is an effective strategy to overcome multiple drug resistance in cancer[30]. Despite promising previous studies showing that the inhibition of P-glycoprotein by pharmacological means can sensitize drug-resistant cells, the ultimate goal of restoring drug sensitivity has met with limited success in clinical trials. Our results indicate that RPN2 is partly responsible for P-glycoprotein–mediated drug resistance in breast cancer and is involved in the regulation of the glycosylation status of P-glycoprotein. In fact, downregulation of *RPN2* restored drug retention, suggesting that P-glycoprotein function is inhibited via suppression of the glycosylation of P-glycoprotein in MCF7-ADR cells. *N*-glycosylation has been shown to contribute to the stability of the P-glycoproteins[31], and it has been reported that reduced glycosylation results in the disappearance of membrane-bound P-glycoprotein, which causes the loss of a multidrug-resistant phenotype[32]. Furthermore, multidrug-resistant cells are hypersensitive to the *N*-linked glycosylation inhibitor tunicamycin, which induces partial inhibition of the glycosylation of GLUT-1, a glucose transporter, and diminishes GLUT-1–mediated transport[33]. Because the amount of MDR1 mRNA was not significantly decreased in MCF7-ADR cells transduced with RPN2 siRNA, it is predicted that RPN2 inhibition may reduce the glycosylation of P-glycoprotein, thereby inducing perturbation of its subcellular localization, inhibition of its protein synthesis and/or acceleration of its degradation, with MCF7-ADR cells inevitably becoming hypersensitive response to docetaxel. In contrast, the RPN2 protein is part of an *N*-oligosaccharyl transferase complex that links to *N*-glycosylation ability; therefore, RPN2 inhibition could affect *N*-oligosaccharyl transferase function, resulting in impaired glycosylation of the P-glycoproteins. We speculate that RPN2 has a key role in drug-resistant tumor cells that overexpress P-glycoprotein and acts as a facilitator, stabilizing factor or both for *N*-glycosylation of P-glycoprotein. The coordinated expression of RPN2 and P-glycoprotein may participate in the mechanism of docetaxel resistance via the glycosylation status of P-glycoprotein.

However, one group has recently reported that the stability of P-glycoprotein is regulated by the ubiquitin-proteasome pathway in multidrug-resistant cancer cells[34]. Furthermore, the P-glycoprotein must be phosphorylated by protein kinase C (PKC) to effectively

function as a drug-efflux pump[35], which suggests that PKC is indirectly involved in the development of the multidrug-resistant phenotype. More recently, it was revealed that wild-type p53, a tumor suppressor, may resensitize soft tissue sarcoma to chemotherapeutic agents by reducing MDR1 phosphorylation via transcriptional repression of PKC expression[36]. There is no direct evidence of RPN2 involvement with the transcriptional repression of PKC. Other transporter proteins mediating drug resistance are the multidrug resistance–associated protein and ABCG2. Whether these different populations of multidrug resistance–associated protein family members and ABCG2 are affected by RPN2 has yet to be determined.

Recently, downregulation of multidrug resistance by the introduction of synthetic siRNAs has been reported[37,38]. However, only partial reversal of the drug-sensitive phenotype of the cells has been obtained. A possible explanation for this low inhibitory effect is that it was the result of a long half-life of P-glycoprotein[39] and the less efficient delivery of synthetic siRNAs into cells. Although the data are not shown, we compared the cell growth inhibition by synthetic RPN2 siRNA versus MDR1 siRNA in the presence of docetaxel *in vitro*. At the mRNA level, the downregulation of RPN2 and MDR1 obtained with the most efficient siRNA was 90% and 80%, respectively. These results indicate that cell growth inhibition was achieved by both siRNAs, although RPN2 siRNA showed a stronger growth inhibitory effect compared to MDR1 siRNA. Thus, though it is impossible at the moment to judge whether MDR1 or RPN2 is a more profitable target for overcoming drug resistance, RPN2 does provide a valuable clue for making multidrug-resistant breast cancer cells sensitive to anticancer drugs.

The continuing interest in apoptosis among cancer biologists has been strengthened by the hope that a molecular understanding of cell death will inform our understanding of cancer drug resistance. In fact, upregulation of antiapoptotic *Bcl2* family genes has been shown to be key in tumor malignancy and drug resistance[40,41]. Overexpression of exogenous Bcl-xL or Bcl-2 suppresses apoptosis[42,43]. In our study, knockdown of RPN2 by siRNA in MCF7-ADR cells selectively downregulated mRNA expression of Bcl-xL and Bcl-w (**Supplementary Fig. 6** online). These results suggest that RPN2 regulates Bcl-xL– and Bcl-w–mediated antiapoptosis and may be partly responsible for the docetaxel resistance of the MCF7-ADR cells. It has already been reported that apoptosis-based therapies[44], such as the downregulation of Bcl-xL expression, Bcl-w expression or both with antisense oligonucleotides, abolish tumorigenicity and enhance chemosensitivity in human malignant glioma cells[45–47]. In addition, Bcl-xL and Bcl-w are upregulated by nuclear factor-κB (NF-κB)[48]. Some chemotherapeutic agents, such as cisplatin and docetaxel, instantly induce the activation of NF-κB in cancer cells, and the cells become drug resistant[49]. In fact, we found that *RPN2* gene expression is also induced by docetaxel treatment of drug-sensitive MCF7 cells. Therefore, it would be useful to know whether RPN2 induces the downregulation of Bcl-xL and Bcl-w in MCF7-ADR cells by direct association with the NF-κB signaling pathway.

It is noteworthy that our findings using docetaxel-resistant human breast cancer cells are commonly found in other multiple cancers. Cisplatin-resistant human non–small cell lung carcinoma cells recover their sensitivity to cisplatin by knockdown of *RPN2* expression and die by apoptosis (Y.Y., K.H. and T.O., unpublished data). In addition, mouse mammary tumor cells resistant to docetaxel express mouse Rpn2, and inhibition of Rpn2 results in apoptotic cell death in the presence of docetaxel (**Supplementary Fig. 2e–g**). Therefore, RPN2 status is responsible for the drug-resistant nature of multiple cancer cell lines both in humans and in mice, and RPN2 expression may confer cross-resistance to a variety of anticancer drugs.

We previously reported that a group of redox genes is useful for the prediction of the clinical response to docetaxel in subjects with breast cancer[16]. Our current results indicate that the RPN2 mRNA level might serve as a predictor of the response to anticancer therapy rather than as a prognostic factor. The determination of the RPN2 mRNA level will be useful in the selection of subjects who are likely to benefit from adjuvant chemotherapy. Furthermore, our animal experiments suggest that treatment of subjects with a pharmacological agent that blocks RPN2 expression or function may induce a complete response to chemotherapeutic drugs. The *RPN2* gene may therefore represent a promising new target for RNAi therapeutics against multidrug-resistant tumors.

METHODS

Cell culture. Human mammary carcinoma cell lines, MCF7 cells and multidrug-resistant MCF7-ADR cells were provided by Shien-Lab, Medical Oncology, National Cancer Center Hospital of Japan. We cultured MCF7, MCF7-ADR and MDA-MB-231 (American Type Culture Collection) cells in RPMI 1640 (Gibco BRL) supplemented with 10% FBS (Gibco BRL) under 5% CO_2 in a humidified incubator at 37 °C. We cultured the mouse mammary tumor cell line EMT6/AR10.0 (European Collection of Cell Cultures), which shows docetaxel resistance, in MEM (EBSS) with 2 mM glutamine, 1% non essential amino acids and 10% FBS. The establishment of bioluminescent MCF7-ADR-Luc cells and docetaxel-resistant MDA-MB-231/MDR1 cells is described in **Supplementary Methods** online.

Design and synthesis of small interfering RNAs. We designed siRNAs and synthesized them with an siRNA duplex for each gene target (Dharmacon) for the preparation of an atelocollagen-based cell transfection array. The siRNA sequences are described in **Supplementary Methods.**

Atelocollagen-based cell transfection array. For RNAi-based functional screening, we prepared an atelocollagen-based cell transfection array, which enables reverse transfection of cells by atelocollagen-mediated gene transfer (**Supplementary Methods**). We performed live-cell luciferase assay for measurement of cell growth, and we performed caspase-7 assays with Apo-ONE Caspase-3/7 Assay Reagent (Promega) and Hoechst staining for apoptosis (**Supplementary Methods**).

Real-time reverse transcription PCR. We purified total RNA from cells and tumor tissues with an RNeasy Mini Kit and RNase-Free DNase Set (QIAGEN) and produced cDNAs with an ExScript RT reagent Kit (Takara). We then subjected cDNA samples to real-time PCR with SYBR Premix Ex Taq (Takara) and specific primers (**Supplementary Methods**). We carried out the reactions in a LightCycler (Roche Diagnostics). We normalized gene expression levels by *HPRT1* or *ACTB*. The cell-direct quantitative RT-PCR method is described in the **Supplementary Methods.**

Atelocollagen-mediated RPN2 small interfering RNA delivery *in vivo*. We performed mouse experiments in compliance with the guidelines of the Institute for Laboratory Animal Research at the National Cancer Center Research Institute of Japan. We used 4-week-old female athymic nude mice (CLEA Japan) to generate an experimental orthotopic breast cancer model. We injected 1.0×10^7 MCF7-ADR cells or MDA-MB-231/MDR1 cells suspended in 100 μl sterile PBS into the fat pad. When the tumor grew to approximately 5 mm in diameter, we injected mice with 200 μl of siRNA-atelocollagen by intratumoral injection. Preparation of the siRNA-atelocollagen complex is described in the **Supplementary Methods.** Simultaneously, we injected docetaxel i.p. into mice. We harvested tumor tissues for analysis of RPN2 mRNA and RPN2 protein at 24 h and 72 h after treatment, respectively.

TUNEL technique. We harvested tumor tissues 72 h after administration of siRNA and prepared frozen sections. We then performed TUNEL staining with an *in situ* Cell Death Detection Kit, Fluorescein (Roche Diagnostics), according to the manufacturer's protocol. We stained the nuclei with DAPI. We

determined the number of fluorescein-positive cells in three microscopic fields of each section by fluorescence microscopy.

Docetaxel disposition in tumors. We studied drug disposition of docetaxel in tumors in mice by HPLC with ultraviolet detection at 225 nm after solid-liquid extraction as described elsewhere[50]. Eleven hours after i.p. administration of 20 mg kg^{-1} docetaxel, we harvested the tumors treated with siRNA-atelocollagen complex and then analyzed the docetaxel abundance in the tumor.

Transfection of small interfering RNA. We carried out transfection of MCF7-ADR and EMT6/AR10.0 cells with siRNA using DharmaFECT 1 (Dharmacon) and TransIT-TKO (Mirus), respectively, according to the manufacturers' protocol (**Supplementary Methods**).

Antibodies. We used RPN2-specific antibody (H300, Santa Cruz Biotechnology) and MDR-specific antibody (G-1, Santa Cruz Biotechnology). We visualized staining with Alexa 488 or Alexa 594 (Molecular Probes). We used fluorescence microscopy or confocal fluorescence microscopy (Olympus) for observation of immunofluorescence-stained cells. The procedures of western blotting and immunofluorescence staining are described in the **Supplementary Methods**.

Rhodamine-123 retention assay. We washed cells once with prewarmed Opti-MEM I medium (37 °C, Gibco BRL) and incubated the cells for 30 min at 37 °C in the Opti-MEM I medium containing 10 μM rhodamine-123. We then removed the rhodamine-123 solution from the extracellular medium and washed the cells twice with Opti-MEM I medium. We observed the cells for fluorescence of rhodamine-123 under fluorescence microscopy.

Human samples. The study protocol for clinical samples (results presented in **Table 1**) was approved by the Institutional Review Board of Osaka University Medical School, and written informed consent was obtained from each subject (**Supplementary Note**).

Statistical analyses. We conducted statistical analysis by analysis of variance with the Student's *t*-test. We considered a P value of 0.05 or less as a significant difference.

Note: Supplementary information is available on the Nature Medicine website.

ACKNOWLEDGMENTS

Human mammary carcinoma cell lines, MCF7 cells and multidrug-resistant MCF7-ADR cells were provided by Shien-Lab, Medical Oncology, National Cancer Center Hospital of Japan. We gratefully thank S. Noguchi for the initiation of the whole project and for helpful discussion. We also thank H. Inaji, K. Yoshioka and K. Itoh for their kind assistance; J. Miyazaki (Osaka University) for the kind gift of CAG promoter; and A. Inoue and M. Wada for their excellent technical work. This work was supported in part by a grant-in-aid for the Third-Term Comprehensive 10-Year Strategy for Cancer Control of Japan; a grant-in-aid for Scientific Research on Priority Areas Cancer from the Japanese Ministry of Education, Culture, Sports, Science and Technology; and the Program for Promotion of Fundamental Studies in Health Sciences of the National Institute of Biomedical Innovation of Japan.

AUTHOR CONTRIBUTIONS

K.H. performed the experimental work, data analysis and writing of the first draft of the manuscript. K.K. and T.O. selected the initial set of genes subjected to the screening. K.I.-K., K.K., T.Y. and T.O. participated in the conception, design and coordination of the study. F.T. and Y.Y. performed siRNA delivery *in vivo* and helped with data analysis. K.N. provided drug-resistant cell lines. S.N. provided delivery molecules. The manuscript was finalized by T.O. with the assistance of all authors.

Published online at http://www.nature.com/naturemedicine/
Reprints and permissions information is available online at http://npg.nature.com/reprintsandpermissions/

1. Kaufmann, M. *et al.* International expert panel on the use of primary (preoperative) systemic treatment of operable breast cancer: review and recommendations. *J. Clin. Oncol.* **21**, 2600–2608 (2003).
2. Gradishar, W.J. *et al.* Neoadjuvant docetaxel followed by adjuvant doxorubicin and cyclophosphamide in patients with stage III breast cancer. *Ann. Oncol.* **16**, 1297–1304 (2005).
3. Formenti, S.C. *et al.* Preoperative twice-weekly paclitaxel with concurrent radiation therapy followed by surgery and postoperative doxorubicin-based chemotherapy in locally advanced breast cancer: A phase I/II trial. *J. Clin. Oncol.* **21**, 864–870 (2003).
4. Engels, F.K., Sparreboom, A., Mathot, R.A. & Verweij, J. Potential for improvement of docetaxel-based chemotherapy: a pharmacological review. *Br. J. Cancer* **93**, 173–177 (2005).
5. Crown, J., O'Leary, M. & Ooi, W.S. Docetaxel & paclitaxel in the treatment of breast cancer: a review of clinical experience. *Oncologist* **9**, 24–32 (2004).
6. Jones, S.E. *et al.* Randomized phase III study of docetaxel compared with paclitaxel in metastatic breast cancer. *J. Clin. Oncol.* **23**, 5542–5551 (2005).
7. Bonneterre, J. *et al.* Efficacy and safety of docetaxel (Taxotere) in heavily pretreated advanced breast cancer patients: the French compassionate use programme experience. *Eur. J. Cancer* **35**, 1431–1439 (1999).
8. Gottesman, M.M., Pastan, I. & Ambudkar, S.V. P-glycoprotein and multidrug resistance. *Curr. Opin. Genet. Dev.* **6**, 610–617 (1996).
9. Duan, Z., Brakora, K.A. & Seiden, M.V. Inhibition of ABCB1 (MDR1) and ABCB4 (MDR3) expression by small interfering RNA and reversal of paclitaxel resistance in human ovarian cancer cells. *Mol. Cancer Ther.* **3**, 833–838 (2004).
10. Leslie, E.M., Deeley, R.G. & Cole, S.P. Toxicological relevance of the multidrug resistance protein 1, MRP1 (ABCC1) and related transporters. *Toxicology* **167**, 3–23 (2001).
11. Renes, J., de Vries, E.G., Jansen, P.L. & Muller, M. The (patho)physiological functions of the MRP family. *Drug Resist. Updat.* **3**, 289–302 (2000).
12. Leonessa, F. & Clarke, R. ATP binding cassette transporters and drug resistance in breast cancer. *Endocr. Relat. Cancer* **10**, 43–73 (2003).
13. Lin, J.C., Chang, S.Y., Hsieh, D.S., Lee, C.F. & Yu, D.S. The association of Id-1, MIF and GSTpi with acquired drug resistance in hormone independent prostate cancer cells. *Oncol. Rep.* **13**, 983–988 (2005).
14. Galimberti, S., Testi, R., Guerrini, F., Fazzi, R. & Petrini, M. The clinical relevance of the expression of several multidrug-resistant-related genes in patients with primary acute myeloid leukemia. *J. Chemother.* **15**, 374–379 (2003).
15. Burg, D., Riepsaame, J., Pont, C., Mulder, G. & van de Water, B. Peptide-bond modified glutathione conjugate analogs modulate GSTpi function in GSH-conjugation, drug sensitivity and JNK signaling. *Biochem. Pharmacol.* **71**, 268–277 (2006).
16. Iwao-Koizumi, K. *et al.* Prediction of docetaxel response in human breast cancer by gene expression profiling. *J. Clin. Oncol.* **23**, 422–431 (2005).
17. Kim, S.J. *et al.* High thioredoxin expression is associated with resistance to docetaxel in primary breast cancer. *Clin. Cancer Res.* **11**, 8425–8430 (2005).
18. Kato, K. Adaptor-tagged competitive PCR: a novel method for measuring relative gene expression. *Nucleic Acids Res.* **25**, 4694–4696 (1997).
19. Honma, K. *et al.* Atelocollagen-based gene transfer in cells allows high-throughput screening of gene functions. *Biochem. Biophys. Res. Commun.* **289**, 1075–1081 (2001).
20. Honma, K., Miyata, T. & Ochiya, T. The role of atelocollagen-based cell transfection array in high-throughput screening of gene functions and in drug discovery. *Curr. Drug Discov. Technol.* **1**, 287–294 (2004).
21. Minakuchi, Y. *et al.* Atelocollagen-mediated synthetic small interfering RNA delivery for effective gene silencing *in vitro* and *in vivo*. *Nucleic Acids Res.* **32**, e109 (2004).
22. Takeshita, F. *et al.* Efficient delivery of small interfering RNA to bone-metastatic tumors by using atelocollagen *in vivo*. *Proc. Natl. Acad. Sci. USA* **102**, 12177–12182 (2005).
23. Ochiya, T. *et al.* New delivery system for plasmid DNA *in vivo* using atelocollagen as a carrier material: the Minipellet. *Nat. Med.* **5**, 707–710 (1999).
24. Ochiya, T., Nagahara, S., Sano, A., Itoh, H. & Terada, M. Biomaterials for gene delivery: atelocollagen-mediated controlled release of molecular medicines. *Curr. Gene Ther.* **1**, 31–52 (2001).
25. Crimaudo, C., Hortsch, M., Gausepohl, H. & Meyer, D.I. Human ribophorins I and II: the primary structure and membrane topology of two highly conserved rough endoplasmic reticulum-specific glycoproteins. *EMBO J.* **6**, 75–82 (1987).
26. Kelleher, D.J., Kreibich, G. & Gilmore, R. Oligosaccharyltransferase activity is associated with a protein complex composed of ribophorins I and II and a 48 kd protein. *Cell* **69**, 55–65 (1992).
27. Kelleher, D.J. & Gilmore, R. An evolving view of the eukaryotic oligosaccharyltransferase. *Glycobiology* **16**, 47R–62R (2006).
28. Loo, T.W., Bartlett, M.C. & Clarke, D.M. The dileucine motif at the COOH terminus of human multidrug resistance P-glycoprotein is important for folding but not activity. *J. Biol. Chem.* **280**, 2522–2528 (2005).
29. Ochiya, T., Honma, K., Takeshita, F. & Nagahara, S. Atelocollagen-mediated drug discovery technology. *Expert Opin. Drug Discov.* **2**, 159–167 (2007).
30. Tsuruo, T. *et al.* Molecular targeting therapy of cancer: drug resistance, apoptosis and survival signal. *Cancer Sci.* **94**, 15–21 (2003).
31. Schinkel, A.H., Kemp, S., Dolle, M., Rudenko, G. & Wagenaar, E. *N*-glycosylation and deletion mutants of the human MDR1 P-glycoprotein. *J. Biol. Chem.* **268**, 7474–7481 (1993).
32. Kramer, R. *et al.* Inhibition of *N*-linked glycosylation of P-glycoprotein by tunicamycin results in a reduced multidrug resistance phenotype. *Br. J. Cancer* **71**, 670–675 (1995).
33. Bentley, J., Quinn, D.M., Pitman, R.S., Warr, J.R. & Kellett, G.L. The human KB multidrug-resistant cell line KB-C1 is hypersensitive to inhibitors of glycosylation. *Cancer Lett.* **115**, 221–227 (1997).
34. Zhang, Z., Wu, J.Y., Hait, W.N. & Yang, J.M. Regulation of the stability of P-glycoprotein by ubiquitination. *Mol. Pharmacol.* **66**, 395–403 (2004).

35. O'Brian, C.A., Ward, N.E., Stewart, J.R. & Chu, F. Prospects for targeting protein kinase C isozymes in the therapy of drug-resistant cancer—an evolving story. *Cancer Metastasis Rev.* **20**, 95–100 (2001).
36. Zhan, M. *et al.* Transcriptional repression of protein kinase Cα via Sp1 by wild type p53 is involved in inhibition of multidrug resistance 1 P-glycoprotein phosphorylation. *J. Biol. Chem.* **280**, 4825–4833 (2005).
37. Nieth, C., Priebsch, A., Stege, A. & Lage, H. Modulation of the classical multidrug resistance (MDR) phenotype by RNA interference (RNAi). *FEBS Lett.* **545**, 144–150 (2003).
38. Wu, H., Hait, W.N. & Yang, J.M. Small interfering RNA–induced suppression of MDR1 (P-glycoprotein) restores sensitivity to multidrug-resistant cancer cells. *Cancer Res.* **63**, 1515–1519 (2003).
39. Muller, C., Laurent, G. & Ling, V. P-glycoprotein stability is affected by serum deprivation and high cell density in multidrug-resistant cells. *J. Cell. Physiol.* **163**, 538–544 (1995).
40. Pommier, Y., Sordet, O., Antony, S., Hayward, R.L. & Kohn, K.W. Apoptosis defects and chemotherapy resistance: molecular interaction maps and networks. *Oncogene* **23**, 2934–2949 (2004).
41. Sordet, O., Khan, Q.A., Kohn, K.W. & Pommier, Y. Apoptosis induced by topoisomerase inhibitors. *Curr. Med. Chem. Anticancer Agents* **3**, 271–290 (2003).
42. Schott, A.F., Apel, I.J., Nunez, G. & Clarke, M.F. Bcl-XL protects cancer cells from p53-mediated apoptosis. *Oncogene* **11**, 1389–1394 (1995).
43. Walczak, H., Bouchon, A., Stahl, H. & Krammer, P.H. Tumor necrosis factor-related apoptosis-inducing ligand retains its apoptosis-inducing capacity on Bcl-2– or Bcl-xL–overexpressing chemotherapy-resistant tumor cells. *Cancer Res.* **60**, 3051–3057 (2000).
44. Reed, J.C. Apoptosis-based therapies. *Nat. Rev. Drug Discov.* **1**, 111–121 (2002).
45. Lytle, R.A., Jiang, Z., Zheng, X. & Rich, K.M. BCNU down-regulates anti-apoptotic proteins Bcl-xL and Bcl-2 in association with cell death in oligodendroglioma-derived cells. *J. Neurooncol.* **68**, 233–241 (2004).
46. Jiang, Z., Zheng, X. & Rich, K.M. Down-regulation of Bcl-2 and Bcl-xL expression with bispecific antisense treatment in glioblastoma cell lines induce cell death. *J. Neurochem.* **84**, 273–281 (2003).
47. Guensberg, P. *et al.* Bcl-xL antisense oligonucleotides chemosensitize human glioblastoma cells. *Chemotherapy* **48**, 189–195 (2002).
48. Tran, N.L. *et al.* The tumor necrosis factor–like weak inducer of apoptosis (TWEAK)-fibroblast growth factor–inducible 14 (Fn14) signaling system regulates glioma cell survival via NFκB pathway activation and BCL-XL/BCL-W expression. *J. Biol. Chem.* **280**, 3483–3492 (2005).
49. Li, Y. *et al.* Inactivation of nuclear factor κB by soy isoflavone genistein contributes to increased apoptosis induced by chemotherapeutic agents in human cancer cells. *Cancer Res.* **65**, 6934–6942 (2005).
50. Vergniol, J.C., Bruno, R., Montay, G. & Frydman, A. Determination of Taxotere in human plasma by a semi-automated high-performance liquid chromatographic method. *J. Chromatogr.* **582**, 273–278 (1992).

Identification of prognostic biomarkers in gastric cancer using endoscopic biopsy samples

Yasuhide Yamada,[1] Tokuzo Arao,[2] Takuji Gotoda,[3] Hirokazu Taniguchi,[4] Ichiro Oda,[3] Kuniaki Shirao,[1] Yasuhiro Shimada,[1] Tetsuya Hamaguchi,[1] Ken Kato,[1] Tetsutaro Hamano,[7] Fumiaki Koizumi,[5] Tomohide Tamura,[1] Daizo Saito,[3] Tadakazu Shimoda,[4] Makoto Saka,[6] Takeo Fukagawa,[6] Hitoshi Katai,[6] Takeshi Sano,[6] Mitsuru Sasako[6] and Kazuto Nishio[2,8]

[1]Medical Oncology, [3]Endoscopic Division, [4]Diagnostic Pathology Division, [5]Shien Lab, and [6]Surgical Division, National Cancer Center Hospital, 5-1-1 Tsukiji, Chuo-ku, Tokyo 104-0045; [2]Department of Genome Biology, Kinki University School of Medicine, 377-2 Ohno-Higashi, Osaka-Sayama, Osaka 589-8511; [7]Hamano Statistical Analysis Ltd, 6-7-15 Chuo-cho, Higashikurume, Tokyo 203-0054, Japan

(Received June 22, 2008/Revised July 16, 2008/Accepted July 16, 2008/Online publication September 28, 2008)

Endoscopic biopsy prior to chemotherapy provides an opportunity for studying biomarkers to predict the overall survival in gastric cancer patients. This prospective study was performed to identify prognostic biomarkers in patients with unresected gastric cancer. Fifty-nine cases of chemotherapy-naive metastatic gastric cancer were enrolled in this study. A microarray analysis was performed using 40 biopsy samples to identify candidate genes whose expressions might be correlated with the overall survival. After adjusting for clinical covariates based on a multivariate analysis, the identified genes were validated using real-time reverse transcription polymerase chain reaction (RT-PCR) analysis in 19 independent validation samples. Ninety-eight candidate genes whose expression levels were significantly correlated with the overall survival were identified using a microarray analysis based on a proportional hazards model ($P < 0.005$). Multivariate analysis was performed to assess 10 of these genes, and the results yielded a statistical significance level for *DACH1* and *PDCD6*. We further evaluated these two genes in independent samples using real-time RT-PCR and found that lower mRNA expression levels of *PDCD6* were correlated significantly with a poor overall survival. We identified *PDCD6* as a prognostic biomarker in patients with unresected gastric cancer using endoscopic biopsy samples. Our PCR-based single gene prediction strategy successfully predicted the overall survival and may lead to a better understanding of this disease subgroup. (*Cancer Sci* 2008; 99: 2193–2199)

Over the past two decades, various anticancer agents have been examined for their efficacy against gastric cancer, including 5-fluorouracil (5-FU) and 5-FU-based drugs, taxanes, CPT-11 and cisplatin, all administered either as monotherapy or in combination regimens;[1] however, the median survival time (MST) of these patients remains at only approximately 7 months.[2,3] In a recent randomized phase III trial examining oral S-1 monotherapy and cisplatin plus irinotecan combination therapy, the response rates to both S-1 and to the cisplatin plus irinotecan combination therapy were approximately 50%, indicating that around half of the patients did not respond to chemotherapy,[4–7] and the MST in both the arms was less than 1 year.[8] Thus, the prognosis of patients with gastric cancer remains poor.

The commonly recognized prognostic factors in cases of unresectable gastric cancer are the performance status, presence/absence of liver metastases, presence/absence of peritoneal metastases and the serum levels of alkaline phosphatase.[9] Many molecular biomarkers have been also investigated for their potential to predict the outcome in hypothesis-based studies. Several studies have shown that the mRNA levels and immunohistochemical staining intensity of thymidylate synthase (TS) in gastric cancers treated with fluorouracil are associated with the response and survival; in addition, the excision repair cross-complementing (ERCC)1 gene expression level has been shown to be associated with the clinical outcome in patients treated with cisplatin.[10,11] HER2 expression has also been reported to be a prognostic marker in cases of differentiated gastric cancer.[12,13] Mutation of p53 and high p53 protein expression, and high expression levels of urokinase-plasminogen activator, xanthine oxidoreductase, claudin-4, vascular endothelial growth factor, interleukin-8 and cyclin E have all been correlated with poor survival.[13–19] In terms of epigenetic alterations, reduced expression of acetylated histone H4 or DNA methylation of CDH1 and RAR-β have been shown to be correlated with tumor invasiveness and the tumor metastasizing potential.[20,21]

On the other hand, the recent introduction of the microarray technology has enabled significant genes to be identified almost throughout the genome using a hypothesis-free approach. The possibility of performing genome-wide searches is a major advantage, and such searches may be the only way to discover genes that would otherwise be unlikely to even be suggested as candidates. In gastric cancer, biopsy samples of the primary lesions can be easily obtained by endoscopy prior to treatment; however, few prospective biomarker studies using endoscopic biopsy samples to predict patient outcome have been performed to date. Therefore, we conducted a prospective study to identify biomarkers for predicting survival in patients with unresected metastatic gastric cancer.

Materials and Methods

Patients and samples. The eligible subjects in this study were patients with histologically confirmed, untreated and metastatic stage IV gastric cancer between 20 and 75 years of age. Additional inclusion criteria included an Eastern Cooperative Oncology Group performance status of 0–2. The exclusion criteria included history of prior chemotherapy or major surgery. All patients received chemotherapy using a 5-FU-based regimen (5-FU alone, S1 alone, 5-FU + methotrexate, 5-FU + cisplatin, or S1 + cisplatin) or a CPT-11 plus cisplatin regimen. Sixty-five gastric cancer patients were enrolled in the study. Of these, two were excluded because of insufficient RNA quantities extracted from their biopsy specimens, and four were excluded because of the poor RNA quality. Thus, samples from the remaining 59 patients were analyzed. The survival time was followed after the patients were initiated on chemotherapy. This study was approved

[8]To whom correspondence should be addressed. E-mail: knishio@med.kindai.ac.jp

doi: 10.1111/j.1349-7006.2008.00935.x

by the Institutional Review Board of the National Cancer Center Hospital, and written informed consent was obtained from all the patients.

The endoscopic biopsy samples collected were immediately placed in an RNA stabilization solution (Isogen; Nippongene, Tokyo, Japan) and stored at −80°C. Other biopsy samples obtained from the same location were reviewed by a pathologist to confirm the presence of tumor cells. The RNA extraction method and the quality check protocol have been described previously.[22]

Study design. This prospective study was started in July 2003 and enrollment was completed in November 2006 at the National Cancer Center Hospital. Fifty-nine gastric cancer samples were evaluated in this study. The samples were divided into a training set ($n = 40$) and a validation set ($n = 19$; 2:1) using computer-generated randomization (Microsoft Office Excel, Microsoft, Redmond, WA, USA). A microarray analysis was performed using the training set of 40 samples, and candidate genes whose expressions were correlated with the overall survival were identified. Multivariate analysis was performed to adjust the expression of 10 of these candidate genes for clinical features. Finally, the significant genes were evaluated in an independent set of 19 samples and survival was predicted using the results of real-time reverse transcription polymerase chain reaction (RT-PCR) analyses.

Real-time RT-PCR. Real-time RT-PCR was performed for 10 genes: *DACH1* (dachshund homolog 1, NM_004392); *EGFR* (epidermal growth factor receptor, NM_005228); *MT1X* (metallothionein 1X, NM_005952); *YWHAE* (tyrosine 3-monooxygenase/tryptophan 5-monooxygenase activation protein, epsilon polypeptide, NM_006761); *GPX3* (glutathione peroxidase 3, NM_002084); *PDCD6* (programmed cell death 6, NM_013232); *WDR33* (WD repeat domain 33, NM_018383); *C14orf43* (chromosome 14 open reading frame 43, NM_194278); *MYLIP* (myosin regulatory light chain interacting protein, NM_013262); and *GKAP1* (G kinase anchoring protein 1, NM_025211). Glyceraldehyde 3 phosphate dehydrogenase (*GAPD*, NM_002046) was used to normalize the expression levels in the subsequent quantitative analyses. RNA was converted to cDNA using a GeneAmp RNA PCR Core kit (Applied Biosystems, Foster City, CA). The transcripts were quantified using the Power SYBR Green PCR Master Mix (Applied Biosystems) and 7900HT Fast Real-time PCR system (Applied Biosystems) and reported relative to the *GAPD* expression levels. The PCR conditions were as follows: one cycle of denaturation at 95°C for 10 min, followed by 40 cycles at 95°C for 15 s and 60°C for 60 s. To amplify the target genes, the following primers were purchased from Takara (Yotsukaichi, Japan): DACH1-FW, 5′-AAG GGC TGC TAA AGC AAT CAG G-3′, and DACH1-RW, 5′-CTT TGT GGC AAA GCG ACA TTA GG-3′; EGFR-FW, 5′-GGT GCG AAT GAC AGT AGC ATT ATG A-3′, and EGFR-RW, 5′-AAA TGG GCT CCT AAC TAG CTG AAT C-3′; MT1X-FW, 5′-TTG ATC GGG AAC TCC TGC TTC T-3′, and MT1X-RW, 5′-ACA CTT GGC ACA GCC GAC A-3′; GPX3-FW, 5′-ATG CCT ACA GGT ATG CGT GAT TG-3′, and GPX3-RW, 5′-TGC AGG CAC ACA GAT GGT ACA-3′; PDCD6-FW, 5′-TCA AGG CCA GAC TAG ATC AGC CTA A-3′, and PDCD6-RW, 5′-GCT GGG ATG AGG CAC ATG AC-3′; YWHAE-FW, 5′-GGC AGA ATT TGC CAC AGG AA-3′, and YWHAE-RW, 5′-ACC TAA GCG AAT AGG ATG CGT TG-3′; WDR33-FW, 5′-ATG CAT GGG CTC TGT CAG TTT C-3′, and WDR33-RW, 5′-GGC TGA TAC CGG GAC AAC ACT AC-3′; C14orf43-FW, 5′-CAG ACT GGC AAG CCT AAC TCC ATA-3′, and C14orf43-RW, 5′-CAA GGC TGT TCC TGT GCT CTG-3′; MYLIP-FW, 5′-ACG TCT ATC TGC CAA CGC ACA C-3′, and MYLIP-RW, 5′-CAG TTC ATG GAA ACA TGC CAA GTC-3′; GKAP1-FW, 5′-TTG CGA ATA AGT TTC GGA GCA TC-3′, and GKAP1-RW, 5′-GCC ACT GCC ACT ATC CAC TTG TAA-3′; GAPD-FW, 5′-GCA CCG TCA AGG CTG AGA AC-3′, and GAPD-RW, 5′-ATG GTG GTG AAG ACG CCA GT-3′.

Oligonucleotide microarray study. The microarray procedure was performed according to the Affymetrix protocols (Santa Clara, CA). In brief, the total RNA extracted from the tumor samples was analyzed using an Agilent 2100 Bioanalyzer (Agilent Technologies, Waldbronn, Germany) for quality check, and cRNA was synthesized using the GeneChip 3′-Amplification Reagents One-Cycle cDNA Synthesis Kit (Affymetrix). The labeled cRNA were then purified and used for construction of the probes. Hybridization was performed using the Affymetrix GeneChip HG-U133 Plus 2.0 array for 16 h at 45°C. The signal intensities were measured using a GeneChip Scanner3000 (Affymetrix) and converted to numerical data using the GeneChip Operating Software, ver. 1 (Affymetrix).

Statistical analysis. The microarray analysis was performed using the BRB Array Tools software ver. 3.3.0 (http://linus.nci.nih.gov/BRB-ArrayTools.html) developed by Dr Richard Simon and Dr Amy Peng. In brief, a log base 2 transformation was applied to the raw microarray data, and global normalization was used to calculate the median over the entire array. Genes were excluded if the percentage of data missing or filtered out exceeded 20%. Genes that passed the filtering criteria were then considered for further analysis. We computed a statistical significance level ($P < 0.005$) for each gene based on a univariate proportional hazards model.

To adjust the expression of 10 genes (*DACH1*, *EGFR*, *MT1X*, *YWHAE*, *GPX3*, *PDCD6*, *WDR33*, *C14orf43*, *MYLIP* and *GKAP1*) for clinical features (age, sex, performance status [PS], number of metastatic sites, received chemotherapy), clinical data and the normalized microarray expression data of the 10 genes were imported into SAS software ver. 9.1.3 (SAS Institute, Cary, NC, USA) and a Cox regression model was constructed for multivariate analysis against each of the variables. The study groups were divided into two groups based on each of the clinical features: age (<65 or ≥65 years), sex (male or female), PS (0 or ≥1), number of metastatic sites (<3 or ≥3), chemotherapy (5-FU-based or CPT11 + CDDP) and expression levels of 10 genes). $P < 0.05$ was considered significant.

Results

Identification of 98 candidate prognosis-related genes using a microarray analysis. The univariate analysis of clinical features including age (<65 or ≥65 years), sex, PS (0 or ≥1), number of metastatic sites (1, 2 or ≥3) and received chemotherapy (5-FU-based or CPT11 + CDDP) were performed for 40 microarray samples (Table 1). There were no significant differences between any of the two groups divided according to age, sex, number of metastatic sites or received chemotherapy; however, significant differences were noted between the two groups divided according to PS ($P = 0.048$).

To identify the candidate prognosis-related genes from amongst over 47 000 transcripts, a microarray analysis was performed for a training set of 40 samples. A total of 21 308 genes passed the filtering criteria and were further analyzed. Ninety-eight genes were significantly correlated with survival, according to a Cox proportional hazards model ($P < 0.005$) (Table 2). Fifty-nine genes were protective genes (hazard ratio, <1), and 39 were risk genes (hazard ratio >1).

A heat-map of the expression values of the 98 selected genes comparing the unfavorable prognosis group (survival time, <180 days) and favorable prognosis group (survival time, ≥180 days) is shown in Fig. 1. Genes are plotted via hierarchical clustering.

Multivariate analysis of prognosis-related genes. Of the 98 candidate genes, we prioritized those that: (i) were selected by overlapping probes; (ii) were novel genes; or (iii) had a lower

doi: 10.1111/j.1349-7006.2008.00935.x

Table 1. Univariate analysis of clinical features

Variable	No. of patients	MST (days)	*P*-value (log-rank test)
Age (years)			
≥65	16	235	0.454
<65	24	250	
Sex			
Male	29	243	0.926
Female	11	267	
PS			
≥1	24	182	0.048
0	16	309	
Metastasis			
1, 2	10	137	0.102
≥3	30	261	
Chemotherapy			
5-FU-based	26	245	0.594
CPT11 + CDDP	14	240	

MST, median survival time; PS, performance status.

P-value according to a Cox proportional hazards model. We selected the following 10 genes of interest for real-time RT-PCR analysis: *DACH1*, *EGFR*, *MT1X*, *YWHAE*, *GPX3*, *PDCD6*, *WDR33*, *C14orf43*, *MYLIP* and *GKAP1*.

To adjust for relevant clinical covariates against these 10 genes, we performed a multivariate analysis (Table 3). The results of the multivariate analysis revealed that high *DACH1* expression and high *PDCD6* expression were significantly correlated with the favorable outcome ($P = 0.0134$ and $P = 0.0015$, respectively). We therefore considered that the *DACH1* and *PDCD6* expressions were independent prognostic markers from the results of the multivariate analysis. Results of microarray data and patient survival in the training set of 40 patients are shown in Fig. 2. The Kaplan–Meier method was used for *DACH1* and *PDCD6*. The low *PDCD6* and *DACH1* expression groups had significantly poorer outcomes ($P < 0.0001$ and $P = 0.0045$).

Validation using real-time RT-PCR in independent samples. The mRNA expression levels of *DACH1* and *PDCD6* were quantified using real-time RT-PCR in 19 independent samples to validate the results of the microarray. While the expression levels of *DACH1* were not correlated with survival, those of *PDCD6* in independent samples were significantly correlated with the survival ($P = 0.007$) (Table 4). The Kaplan–Meier method was used to estimate the overall survival using the median value (Fig. 3a). All quantified expression levels of real time RT-PCR data are shown as Fig. 3(b). The mRNA expressions of *PDCD6* varied by approximately 25 fold (range, 0.98–25.1). The low *PDCD6* expression groups had significantly poorer outcomes ($P = 0.0018$). We concluded that *PDCD6* was a valuable gene for predicting the survival in patients with gastric cancer. These results indicate that our PCR-based single gene prediction strategy using endoscopic biopsy samples could successfully predict the overall patient survival.

Discussion

Several studies have identified prognostic biomarkers in cases of gastric cancer using microarray analysis. Hasegawa *et al.* identified 12 genes that were associated with lymph node metastasis.[23] Hippo *et al.* identified several genes associated with lymph node metastasis, including Oct-2, and genes associated with the histological type, including liver-intestine cadherin.[24] These studies introduced a novel direction in which microarray analysis could be used to predict postoperative recurrences. Inoue *et al.* selected 78 genes that were differentially expressed between aggressive and non-aggressive cancers and constructed a prognostic scoring system.[25] Leung *et al.* found that high CCL18 expression levels were associated with prolonged overall and disease-free survival.[26] They also found that phospholipase A2 group IIA expression in gastric adenocarcinoma was associated with prolonged survival and less frequent metastasis.[27] Chen *et al.* demonstrated a survival prediction model consisting of three genes (*CD36*, *SLAM*, *PIM-1*) that was capable of predicting poor or good survival in 23 (76.7%) of 30 newly enrolled patients.[28] Most of these studies used surgical specimens to predict postsurgical survival and were conducted retrospectively. Thus, we think that our present prospective study is unique in that we used endoscopic biopsy samples to predict the survival time in patients with unresectable gastric cancer. In patients with unresectable cancer, endoscopic biopsy samples may be the most appropriate specimens available non-invasively for microarray analysis. Although tumor heterogeneity may pose problems when biopsy samples are used as representative tissue specimens and further investigation is required, we believe that endoscopic biopsy samples should continue to be used for microarray analyses. Current clinical study has been confronted with a number of obstacles. Microarray analysis for clinical studies, in particular, has been hampered with bottlenecks such as RNA quality, the extremely large number of genes to be analyzed, an immature analytical tool or methodology and so on. There are two types of obstacles: controllable obstacles and uncontrollable ones. One uncontrollable obstacle is a complex chemotherapy regimen. It is easy to say that a clinical biomarker study should be performed in one particular regimen. Chemotherapy regimen has, however, progressed and become more sophisticated in a short range of time. This study was prospective clinical study and was largely followed by a guideline, Recommendations for Tumor Marker Prognostic Studies (REMARK). To minimize

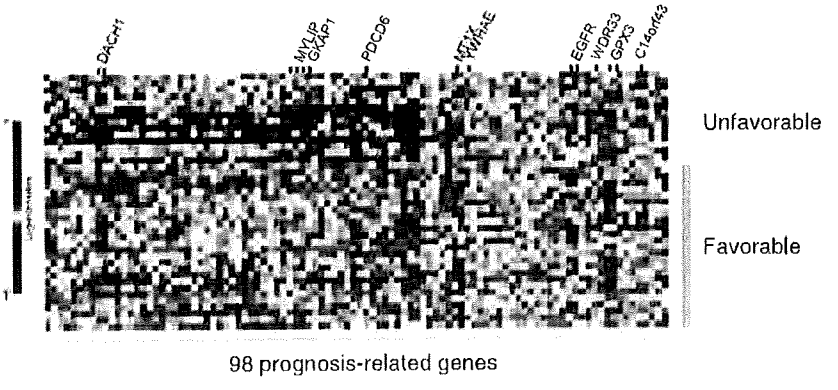

Fig. 1. Heat map of expression values for microarray identifying 98 genes whose expressions were correlated with survival. The hierarchical clustering of the 98 genes comparing the unfavorable prognosis group (survival time, <180 days) and favorable prognosis group (survival time, ≥180 days) is shown. The blue or red colors of each block represent the normalized gene expression levels. Each row represents a sample, and each column represents a gene. The 10 genes included in the multivariate analysis (Table 3) are shown.

Table 2. Prognosis-related genes identified using microarray analysis

P-value	Hazard ratio	Description	Gene	Probe set	Pass	PCR		
0.0002	1.8	Epidermal growth factor receptor	*EGFR*	201984_s_at	2	PCR	1	0.1
0.0005	0.1	DEAD (Asp-Glu-Ala-Asp) box polypeptide 54	*DDX54*	219111_s_at			2	0.1
0.0005	0.5	Chimerin (chimaerin) 2	*CHN2*	213385_at			3	0.1
0.0005	6.1	Ubiquitin-like domain containing CTD phosphatase 1	*UBLCP1*	227413_at			4	0.2
0.0006	0.5	PTK2 protein tyrosine kinase 2	*PTK2*	241387_at			5	0.2
0.0008	3.4	Der1-like domain family, member 2	*DERL2*	218333_at			6	0.2
0.0008	0.5	Leucine rich repeat containing 14	*LRRC14*	32062_at			7	0.2
0.0009	4.5	WD repeat domain 33	*WDR33*	222763_s_at		PCR	8	0.2
0.0009	0.1	Rhomboid domain containing 3	*RHBDD3*	217622_at			9	0.2
0.001	0.3	Myosin regulatory light chain interacting protein	*MYLIP*	228098_s_at	3	PCR	10	0.2
0.0013	4.7	Chromosome 14 open reading frame 43	*C14orf43*	225980_at		PCR	11	0.2
0.0013	0.2	BCL6 co-repressor	*BCOR*	223915_at			12	0.2
0.0013	0.5	MAD1 mitotic arrest deficient-like 1 (yeast)	*MAD1L1*	233921_s_at			13	0.2
0.0013	4.9	Chromosome 14 open reading frame 109	*C14orf109*	213246_at			14	0.2
0.0014	4.2	Hypothetical protein LOC124512	*LOC124512*	225808_at			15	0.2
0.0014	5.0	Ring finger protein 167	*RNF167*	212047_s_at			16	0.2
0.0014	0.6	Hypothetical LOC25845	*LOC25845*	225457_s_at			17	0.2
0.0014	4.2	General transcription factor II, i	*GTF2I*	232710_at			18	0.3
0.0014	0.2	Rho guanine nucleotide exchange factor (GEF) 10-like	*ARHGEF10L*	1570511_at			19	0.3
0.0014	0.3	G kinase anchoring protein 1	*GKAP1*	229312_s_at		PCR	20	0.3
0.0015	1.9	Glutathione peroxidase 3 (plasma)	*GPX3*	214091_s_at	2	PCR	21	0.3
0.0016	0.5	Dachshund homolog 1 (*Drosophila*)	*DACH1*	1567101_at	2	PCR	22	0.3
0.0016	0.3	Diacylglycerol kinase, theta 110kDa	*DGKQ*	226605_at			23	0.3
0.0017	0.6	Hepatocellular carcinoma-associated antigen 112	*HCA112*	218345_at			24	0.3
0.0018	3.5	Mediator of RNA polymerase II transcription, subunit 31 homolog	*MED31*	222867_s_at			25	0.3
0.0018	6.9	Tyrosine 3-monooxygenase/tryptophan 5-monooxygenase activation protein, epsilon polypeptide	*YWHAE*	210317_s_at		PCR	26	0.3
0.0018	0.1	KH domain containing, RNA binding, signal transduction associated 1	*KHDRBS1*	201488_x_at			27	0.3
0.0019	0.3	Solute carrier family 25 (mitochondrial carrier; Graves disease autoantigen), member 16	*SLC25A16*	210686_x_at			28	0.3
0.0019	4.9	Hypothetical protein LOC51255	*LOC51255*	223064_at			29	0.3
0.002	0.2	Cyclin L2 /// similar to Aurora kinase A-interacting protein	*CCNL2 /// LOC643556*	222999_s_at			30	0.3
0.002	7.4	Lectin, mannose-binding, 1	*LMAN1*	224629_at			31	0.3
0.002	0.2	Erythrocyte membrane protein band 4.1 like 4A	*EPB41L4A*	228259_s_at			32	0.3
0.0022	0.2	KIAA0999 protein	*KIAA0999*	204155_s_at			33	0.3
0.0022	0.5	ELOVL family member 7	*ELOVL7*	227180_at			34	0.3
0.0023	4.0	Churchill domain containing 1	*CHURC1*	233268_s_at			35	0.4
0.0024	4.0	Yippee-like 2 (*Drosophila*)	*YPEL2*	227020_at			36	0.4
0.0024	5.9	Hermansky–Pudlak syndrome 1	*HPS1*	210112_at			37	0.4
0.0025	0.3	Hypothetical protein LOC285831	*LOC285831*	228857_at			38	0.4
0.0026	3.5	CDC37 cell division cycle 37 homolog (*Saccharomyces cerevisiae*)-like 1	*CDC37L1*	219343_at			39	0.4
0.0026	2.1	Ankyrin repeat and SOCS box-containing 9	*ASB9*	205673_s_at			40	0.4
0.0026	0.2	Hypothetical gene supported by AK125149	*LOC401577*	239247_at			41	0.5
0.0026	0.3	TBC1 domain family, member 23	*TBC1D23*	236755_at			42	0.5
0.0026	0.3	MRNA full length insert cDNA clone EUROIMAGE 2362292		235505_s_at			43	0.5
0.0026	0.4	Dehydrogenase/reductase (SDR family) member 8	*DHRS8*	217989_at			44	0.5
0.0026	0.4	Nuclear receptor coactivator 2	*NCOA2*	242369_x_at			45	0.5
0.0026	0.2	MRNA; cDNA DKFZp667E0114 (from clone DKFZp667E0114)		235660_at			46	0.5
0.0027	0.4	Transforming, acidic coiled-coil containing protein 1	*TACC1*	242290_at			47	0.5
0.0027	0.2	POU domain, class 2, transcription factor 1	*POU2F1*	1562280_at			48	0.5
0.0027	2.9	p21(CDKN1A)-activated kinase 6	*PAK6*	1555310_a_at				0.5
0.0027	0.5	Mannosyl (alpha-1,3-)-glycoprotein β-1,4-N-acetylglucosaminyltransferase, isozyme A	*MGAT4A*	226039_at			50	0.5
0.0027	5.1	Zinc finger CCCH-type containing 14	*ZC3H14*	204216_s_at			51	0.5
0.0028	0.5	Acyl-CoA synthetase short-chain family member 2	*ACSS2*	235805_at			52	0.5
0.0028	0.3	Programmed cell death 6	*PDCD6*	222380_s_at		PCR	53	0.6
0.0029	3.8	ERGIC and golgi 2	*ERGIC2*	226422_at			54	0.6
0.0029	0.4	Erythrocyte membrane protein band 4.1 like 5	*EPB41L5*	225855_at			55	0.6
0.003	6.5	Chromosome 14 open reading frame 32	*C14orf32*	212644_s_at			56	0.6

doi: 10.1111/j.1349-7006.2008.00935.x

Table 2. *(Continued)*

P-value	Hazard ratio	Description	Gene	Probe set	Pass	PCR		
0.0031	0.2	Transcribed locus		239437_at			57	1.8
0.0031	0.3	DOT1-like, histone H3 methyltransferase (*S. cerevisiae*)	*DOT1L*	231297_at			58	1.9
0.0031	2.2	Transcription elongation factor A (SII)-like 8	*TCEAL8*	224819_at			59	1.9
0.0031	0.3	Laminin, β 1	*LAMB1*	236437_at			60	2.0
0.0032	2.7	FK506 binding protein 5	*FKBP5*	224840_at			61	2.0
0.0033	0.5	Integrin, α 6	*ITGA6*	244665_at			62	2.1
0.0034	2.7	COMM domain containing 9	*COMMD9*	218072_at			63	2.2
0.0034	0.2	Eukaryotic translation initiation factor 4 γ, 3	*EIF4G3*	201936_s_at			64	2.3
0.0035	0.5	235616_at	*235616_at*	235616_at			65	2.6
0.0036	1.9	Metallothionein 1X	*MT1X*	204326_x_at		PCR	66	2.6
0.0036	2.7	Peroxiredoxin 5	*PRDX5*	1560587_s_at			67	2.7
0.0037	0.3	Core-binding factor, runt domain, α subunit 2; translocated to, 2	*CBFA2T2*	207625_s_at			68	2.7
0.0037	0.4	Transcribed locus, moderately similar to XP_531878.2		230168_at			69	2.7
0.0038	0.3	Zinc finger protein 346	*ZNF346*	236267_at			70	2.8
0.0038	2.0	Metallothionein 1H-like protein /// hypothetical protein LOC650610	*LOC645745 /// LOC650610*	211456_x_at			71	2.9
0.0039	0.2	Hypothetical protein DKFZp586I1420	*DKFZp586I1420*	213546_at			72	3.4
0.0039	2.0	Adrenergic, β-2-, receptor, surface	*ADRB2*	206170_at			73	3.5
0.0039	0.3	CTD-binding SR-like protein rA9	*KIAA1542*	234952_s_at			74	3.5
0.0039	2.6	Peroxiredoxin 5	*PRDX5*	222994_at			75	3.6
0.004	0.2	ATPase, H^+ transporting, lysosomal 42kDa, V1 subunit C1	*ATP6V1C1*	226463_at			76	3.8
0.004	8.0	XK, Kell blood group complex subunit-related family, member 8	*XKR8*	218753_at			77	3.8
0.004	0.3	Caspase 6, apoptosis-related cystein peptidase	*CASP6*	242323_at			78	4.0
0.0041	0.4	Coagulation factor XII (Hageman factor)	*F12*	205774_at			79	4.0
0.0041	0.3	Centaurin, γ 2	*CENTG2*	240758_at			80	4.2
0.0042	0.6	LR8 protein	*LR8*	220532_s_at			81	4.2
0.0042	0.2	WD repeat domain 42A	*WDR42A*	243318_at			82	4.5
0.0042	2.6	Potassium channel tetramerisation domain containing 14	*KCTD14*	219545_at			83	4.7
0.0043	2.8	6-Phosphogluconolactonase	*PGLS*	218388_at			84	4.9
0.0044	3.8	Bruno-like 6, RNA binding protein (*Drosophila*)	*BRUNOL6*	227775_at			85	4.9
0.0044	2.3	Zinc finger protein 415	*ZNF415*	205514_at			86	5.0
0.0045	0.5	HIR histone cell cycle regulation defective homolog A (*S. cerevisiae*)	*HIRA*	240451_at			87	5.1
0.0046	0.5	Cardiolipin synthase 1	*CRLS1*	241741_at			88	5.9
0.0046	0.3	c-mer proto-oncogene tyrosine kinase	*MERTK*	233079_at			89	6.1
0.0047	0.2	Additional sex combs like 2 (*Drosophila*)	*ASXL2*	218659_at			90	6.5
0.0047	3.6	Platelet endothelial aggregation receptor 1	*PEAR1*	228618_at			91	6.9
0.0047	0.3	Core-binding factor, runt domain, α subunit 2; translocated to, 2	*CBFA2T2*	238549_at			92	7.4
0.005	0.6	Lysosomal associated protein transmembrane 4 β	*LAPTM4B*	208029_s_at			93	8.0

Pass, number of overlapped probes; PCR, the genes that were subsequently examined using real-time RT-PCR.

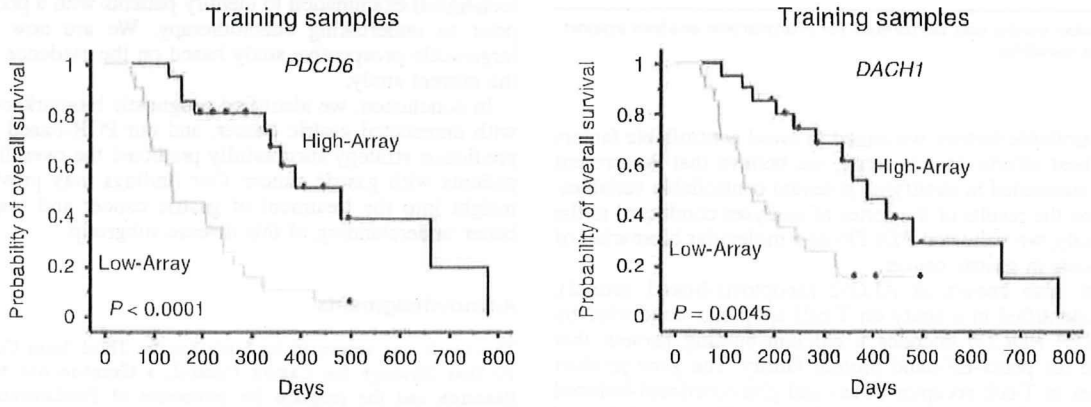

Fig. 2. Results of microarray data and patient survival in the training set of 40 patients. The Kaplan–Meier method was used for *DACH1* and *PDCD6*. The patients were divided into high and low expression groups by median values. The low *PDCD6* and *DACH1* expression groups had significantly poorer outcomes ($P < 0.0001$ and $P = 0.0045$). High-Array, group with high expression levels as determined by signal intensity of microarray data. Low-Array, group with low expression levels as determined by signal intensity of microarray data.

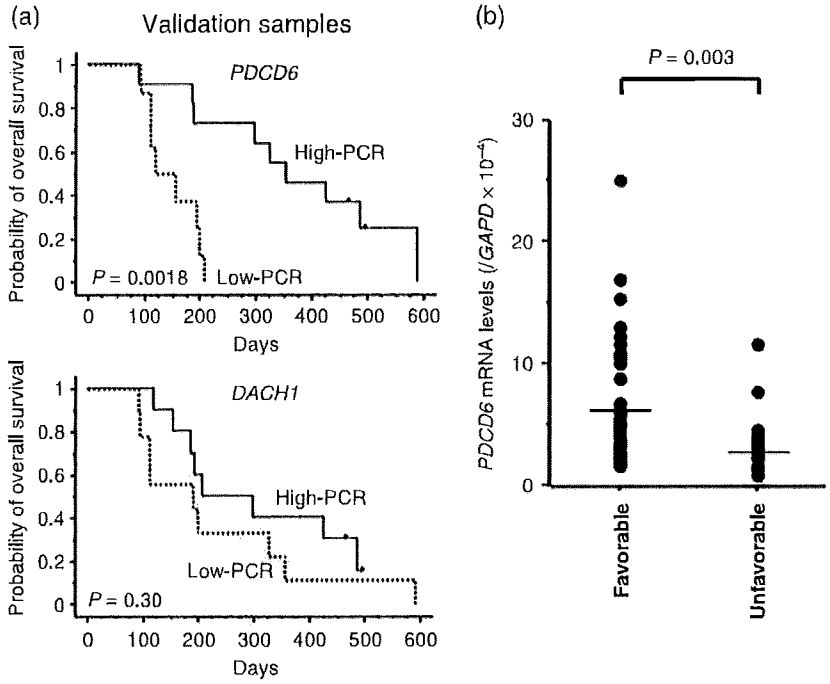

Fig. 3. Results of real-time reverse transcription polymerase chain reaction (RT-PCR) analysis and patient survival in the independent validation set of 19 samples. (a) The Kaplan–Meier method was used to estimate the overall survival. The low *PDCD6* expression groups had significantly poorer outcomes ($P = 0.0018$). High-PCR, group with high expression levels as determined by PCR. Low-PCR, group with low expression levels as determined by PCR. (b) All quantified expression levels of real time RT-PCR data are shown. The mRNA expressions of *PDCD6* were significantly lower in unfavorable group ($P = 0.003$) and varied ~25 fold (range, 0.98–25.1). Favorable, the patients with survival time over 180 days. Unfavorable, the patients with a survival time less than 180 days.

Table 3. Multivariate analysis of prognosis-related genes

Variable	Hazard ratio	95% confidence interval	*P*-value
Age (≥65)	1.78	0.570–5.559	0.3212
Sex (male)	3.26	0.732–14.489	0.1210
Performance status (≥1)	2.36	0.687–8.078	0.1728
Metastasis (≥3)	1.58	0.450–5.561	0.4739
Chemotherapy (5-FU)	1.48	0.402–5.475	0.5541
DACH1	0.38	0.175–0.817	0.0134
EGFR	1.41	0.992–2.001	0.0553
MT1X	0.71	0.317–1.600	0.4111
YWHAE	1.91	0.401–9.061	0.4169
GPX3	1.62	0.869–3.007	0.1293
PDCD6	0.06	0.010–0.334	0.0015
WDR33	1.38	0.268–7.067	0.7017
C14orf43	0.64	0.122–3.407	0.6045
MYLIP	0.67	0.221–2.042	0.4826
GKAP1	2.31	0.751–7.106	0.1440

Cox regression model was performed for multivariate analysis against each of the variables.

Table 4. Results of real-time *RT-PCR* for *PDCD6* and *DACH1* in an independent valiation set

Genes	Hazard ratio	95% confidence limits		*P*-value
		Upper	Lower	
*PDCD6**	0.29	0.12	0.71	0.007
DACH1	0.79	0.56	1.13	0.199

*, $P < 0.05$.

the uncontrollable factors, we aimed to avoid controllable factors with our best efforts. In this sense, we believe that the present study has succeeded in stratifying potential controllable variables.

Based on the results of the series of analyses conducted in the current study, we validated *PDCD6* as a molecular biomarker of the prognosis in gastric cancer.

PDCD6, also known as ALG-2 (apoptosis-linked gene-2), was first identified in a study on T-cell apoptosis conducted by Vito *et al.*[29] *PDCD6* encodes a calcium-binding protein that belongs to the penta-EF-hand protein family. The gene product participates in T-cell receptor-, Fas- and glucocorticoid-induced programmed cell death and cell proliferation. The stimulation of cells to enter the cell cycle is thought to drive the cellular apoptotic program, and the presence of additional survival or pro-apototic signals determines whether a cell proliferates or commits suicide. Krebs *et al.* indicated that the deregulation of such an obviously delicate balance could lead to pathological developments, such as cancer.[30] Detailed biological function of *PDCD6* genes in gastric cancer is still unclear. The speculated function may lead us to hypothesize that the expression is generally downregulated in cancer.

Our ultimate goal is to use real-time RT-PCR or immunohistochemical examination to identify patients with a poor prognosis prior to undertaking chemotherapy. We are now planning a large-scale prospective study based on the evidence obtained in the current study.

In conclusion, we identified prognostic biomarkers in patients with unresected gastric cancer, and our PCR-based single gene prediction strategy successfully predicted the overall survival of patients with gastric cancer. Our findings may provide a novel insight into the treatment of gastric cancer and may lead to a better understanding of this disease subgroup.

Acknowledgments

This work was supported by funds for the Third Term Comprehensive 10-Year Strategy for Cancer Control, a Grant-in-Aid for Scientific Research and the program for promotion of Fundamental Studies in Health Sciences of the National Institute of Biomedical Innovation (NiBio). The following people have played very important roles in the conduct of this project: Hiromi Orita, Hisanao Hamanaka, Ayumu Goto, Hisateru Yasui, Junichi Matsubara, Natsuko Okita, Takako Nakajima,

doi: 10.1111/j.1349-7006.2008.00935.x

Atsuo Takashima, Kei Muro, Takashi Ura, Hideko Morita, Mari Araake, Hisao Fukumoto, Tatsu Shimoyama, Naoki Hayama, Masayuki Takeda, Hideharu Kimura, Kazuko Sakai, Terufumi Kato and Jun-ya Fukai. We also thank Dr Richard Simon and Dr Amy Peng for providing us with the BRB ArrayTools software. This free software was very useful and has been developed for user-friendly applications.

References

1 Sastre J, Garcia-Saenz JA, Diaz-Rubio E. Chemotherapy for gastric cancer. *World J Gastroenterol* 2006; **12**: 204–13.
2 Vanhoefer U, Rougier P, Wilke H *et al.* Final results of a randomized phase III trial of sequential high-dose methotrexate, fluorouracil, and doxorubicin versus etoposide, leucovorin, and fluorouracil versus infusional fluorouracil and cisplatin in advanced gastric cancer: a trial of the European Organization for Research and Treatment of Cancer Gastrointestinal Tract Cancer Cooperative Group. *J Clin Oncol* 2000; **18**: 2648–57.
3 Ohtsu A, Shimada Y, Shirao K *et al.* Randomized phase III trial of fluorouracil alone versus fluorouracil plus cisplatin versus uracil and tegafur plus mitomycin in patients with unresectable, advanced gastric cancer: The Japan Clinical Oncology Group Study (JCOG9205). *J Clin Oncol* 2003; **21**: 54–9.
4 Sakata Y, Ohtsu A, Horikoshi N, Sugimachi K, Mitachi Y, Taguchi T. Late phase II study of novel oral fluoropyrimidine anticancer drug S-1 (1M tegafur-0.4M gimestat-1M otastat potassium) in advanced gastric cancer patients. *Eur J Cancer* 1998; **34**: 1775–20.
5 Koizumi W, Kurihara M, Nakano S, Hasegawa K. Phase II study of S-1, a novel derivative of 5-fluorouracil, in advanced gastric cancer. *Oncology* 2000; **58**: 191–7.
6 Shirao K, Shimada Y, Kondo H *et al.* Phase I–II study of irinotecan hydrochloride combined with cisplatin in patients with advanced gastric cancer. *J Clin Oncol* 1997; **15**: 921–7.
7 Boku N, Ohtsu A, Shimada Y *et al.* Phase II study of combination of irinotecan and cisplatin against metastatic gastric cancer. *J Clin Oncol* 1999; **17**: 319–23.
8 Boku N, Yamamoto S, Shirao K *et al.* Gastrointestinal Oncology Study Group/Japan Clinical Oncology Group. Randomized phase III study of 5-fluorouracil (5-FU) alone versus combination of irinotecan and cisplatin (CP) versus S-1 alone in advanced gastric cancer (JCOG9912) (Abstract). *Proc Am Soc Clin Oncol* 2007; **25**: 18S.
9 Chau I, Norman AR, Cunningham D, Waters JS, Oates J, Ross PJ. Multivariate prognostic factor analysis in locally advanced and metastatic esophago-gastric cancer – pooled analysis from three multicenter, randomized, controlled trials using individual patient data. *J Clin Oncol* 2004; **22**: 2395–403.
10 Metzger R, Leichman CG, Danenberg KD *et al.* ERCC1 mRNA levels complement thymidylate synthase mRNA levels in predicting response and survival for gastric cancer patients receiving combination cisplatin and 5-fluorouracil chemotherapy. *J Clin Oncol* 1998; **16**: 309–16.
11 Boku N, Chin K, Hosokawa K *et al.* Biological makers as a predictor for response and prognosis of unresectable gastric cancer patients treated with 5-fluorouracil and cis-platinum. *Clin Cancer Res* 1998; 4: 1469–74.
12 Yonemura Y, Ninomiya I, Yamaguchi A *et al.* Evaluation of immunoreactivity for erbB-2 protein as a marker of poor short term prognosis in gastric cancer. *Cancer Res* 1991; **51**: 1034–8.
13 Sanz-Ortega J, Steinberg SM, Moro E *et al.* Comparative study of tumor angiogenesis and immunohistochemistry for p53, c-ErbB2, c-myc and EGFr as prognostic factors in gastric cancer. *Histol Histopathol* 2000; **15**: 455–62.
14 Shibata A, Parsonnet J, Longacre TA *et al.* CagA status of *Helicobacter pylori* infection and p53 gene mutations in gastric adenocarcinoma. *Carcinogenesis* 2002; **23**: 419–24.
15 Okusa Y, Ichikura T, Mochizuki H. Prognostic impact of stromal cell-derived urokinase-type plasminogen activator in gastric carcinoma. *Cancer* 1999; **85**: 1033–8.
16 Linder N, Haglund C, Lundin M *et al.* Decreased xanthine oxidoreductase is a predictor of poor prognosis in early-stage gastric cancer. *J Clin Pathol* 2006; **59**: 965–71.
17 Resnick MB, Gavilanez M, Newton E *et al.* Claudin expression in gastric adenocarcinomas: a tissue microarray study with prognostic correlation. *Hum Pathol* 2005; **36**: 886–92.
18 Kido S, Kitadai Y, Hattori N *et al.* Interleukin 8 and vascular endothelial growth factor – prognostic factors in human gastric carcinomas? *Eur J Cancer* 2001; **37**: 1482–7.
19 Xiangming C, Natsugoe S, Takao S *et al.* The cooperative role of p27 with cyclin E in the prognosis of advanced gastric carcinoma. *Cancer* 2000; **89**: 1214–9.
20 Yasui W, Oue N, Ono S, Mitani Y, Ito R, Nakayama H. Histone acetylation and gastrointestinal carcinogenesis. *Ann NY Acad Sci* 2003; **983**: 220–31.
21 Oue N, Motoshita J, Yokozaki H *et al.* Distinct promoter hypermethylation of p16INK4a, CDH1, and RAR-beta in intestinal, diffuse-adherent, and diffuse-scattered type gastric carcinomas. *J Pathol* 2002; **198**: 55–9.
22 Yamanaka R, Arao T, Yajima N *et al.* Identification of expressed genes characterizing long-term survival in malignant glioma patients. *Oncogene* 2006; **25**: 5994–6002.
23 Hasegawa S, Furukawa Y, Li M *et al.* Genome-wide analysis of gene expression in intestinal-type gastric cancers using a complementary DNA microarray representing 23 040 genes. *Cancer Res* 2002; **62**: 7012–17.
24 Hippo Y, Taniguchi H, Tsutsumi S *et al.* Global gene expression analysis of gastric cancer by oligonucleotide microarrays. *Cancer Res* 2002; **62**: 233–40.
25 Inoue H, Matsuyama A, Mimori K, Ueo H, Mori M. Prognostic score of gastric cancer determined by cDNA microarray. *Clin Cancer Res* 2002; **8**: 3475–9.
26 Leung SY, Yuen ST, Chu KM *et al.* Expression profiling identifies chemokine (C-C motif) ligand 18 as an independent prognostic indicator in gastric cancer. *Gastroenterology* 2004; **127**: 457–69.
27 Leung SY, Chen X, Chu KM *et al.* Phospholipase A2 group IIA expression in gastric adenocarcinoma is associated with prolonged survival and less frequent metastasis. *Proc Natl Acad Sci USA* 2002; **99**: 16203–8.
28 Chen CN, Lin JJ, Chen JJ *et al.* Gene expression profile predicts patient survival of gastric cancer after surgical resection. *J Clin Oncol* 2005; **23**: 7286–95.
29 Vito P, Lacana E, D'Adamio L. Interfering with apoptosis: $Ca^{(2+)}$-binding protein ALG-2 and Alzheimer's disease gene ALG-3. *Science* 1996; **271**: 521–5.
30 Krebs J, Saremaslani P, Caduff R. ALG-2: a Ca^{2+}-binding modulator protein involved in cell proliferation and in cell death. *Biochim Biophys Acta* 2002; 1600: 68–73.

Phase III comparative study of a second generation regimen and third generation regimens with concurrent thoracic radiotherapy in patients with unresectable stage III non-small-cell lung cancer: West Japan Oncology Group WJTOG0105.

Nobuyuki Yamamoto[1,2], Kazuhioko Nakagawa[1], Yasumasa Nishimura[1], Kayoko Tsujino[3], Miyako Satouchi[3], Shinzoh Kudoh[4], Toyoaki Hida[5], Masaaki Kawahara[6], Koji Takeda[7], Nobuyuki Katakami[8], Toshiyuki Sawa[9], Soichiro Yokota[10], Takashi Seto[11], Fumio Imamura[12], Hideo Saka[13], Yasuo Iwamoto[14], Hiroshi Semba[15], Yasutaka Chiba[1], Hisao Uejima[1], Masahiro Fukuoka[1]

1: Kinki University Hospital, Osaka-Sayama, Japan;

2: Shizuoka Cancer Center, Naga-izumi, Japan;

3: Hyogo Cancer Center, Akashi, Japan;

4: Osaka City University Hospital, Osaka, Japan;

5: Aichi Cancer Center Hospital, Nagoya, Japan;

6: Kinki-chuo Chest Medical Centre, Sakai, Japan

7: Osaka City General Hospital, Osaka, Japan

8: Kobe City Medical Center General Hospital, Kobe, Japan

9: Gifu Municipal Hospital, Gifu, Japan

10: Toneyama National Hospital, Toyonaka, Japan

11: Tokai University Hospital, Isehara, Japan

12: Osaka Medical Center for Cancer and Cardiovascular Diseases, Osaka, Japan

13: Nagoya Medical Center, Nagoya, Japan

14: Hiroshima City Hospital, Hiroshima, Japan

15: Kumamoto Regional Medical Center, Kumamoto, Japan

Correspondence to Nobuyuki Yamamoto, M.D., Chief, Thoracic Oncology Division, Shizuoka Cancer Center

Address: 1007 Naga-izumicho Shimonagakubo, Sunto-gun, Shizuoka, 411-8777, Japan

E-mail address: n.yamamoto@scchr.jp

Tel: +81-(0)55-989-5222 FAX: +81-(0)55-989-5634

Running head: Phase III study of concurrent chemoradiotherapy compared with 2nd and 3rd generation regimens.

Conflicts of interest: The authors have no potential conflicts of interest to declare.

Presented in part at the 45th Annual Meeting of the American Society of Clinical Oncology, May 29-June 2, 2009, Orlando, FL

This study is registered with UMIN-CTR [http://www.umin.ac.jp/ctr/index.htm, identification number C000000087.

ABSTRACT

Purpose: This phase III trial of concurrent thoracic radiotherapy (TRT) was conducted to compare third generation chemotherapy with second generation chemotherapy in patients with unresectable stage III non-small cell lung cancer (NSCLC).

Patients and Methods: Eligible patients received the following treatments: A (control): four cycles of mitomycin (8 mg/m^2 on day 1) / vindesine (3 mg/m^2 on days 1, 8) / cisplatin (80 mg/m^2 on day 1) + TRT 60 Gy (treatment break for one week); B: weekly irinotecan (20 mg/m^2) / carboplatin (AUC 2) for 6 weeks + TRT 60 Gy, followed by 2 courses of irinotecan (50 mg/m^2 on days1, 8) / carboplatin (AUC 5 on day1); C: weekly paclitaxel (40 mg/m^2) / carboplatin (AUC 2) for 6 weeks + TRT 60 Gy, followed by 2 courses of paclitaxel (200 mg/m^2 on day1) / carboplatin (AUC 5 on day 1).

Results: The median survival time and 5-year survival rate were 20.5, 19.8, 22.0 months and 17.5, 17.8, 19.8% in A, B and C, respectively. Although no significant differences in the OS were apparent among the treatment arms, non-inferiority of the experimental arms was not achieved. The incidences of grade 3/4 neutropenia, febrile neutropenia, and gastrointestinal disorder were

significantly higher in A than in B or C ($p<.001$). Chemotherapy interruptions were more common in B than in A or C.

Conclusions: C exhibited equally efficacious and a more favorable toxicity profile among three arms. C should be considered a standard regimen in the management of locally advanced unresectable NSCLC.

INTRODUCTION

Lung cancer remains the leading cause of cancer-related deaths worldwide[1]. Non-small cell lung cancer (NSCLC) accounts for 80% of all lung cancer cases, and approximately 30% of NSCLC patients present with locally advanced lung cancer[2].

The standard treatment for stage III locally advanced NSCLC was a combined modality of thoracic radiotherapy (TRT) and chemotherapy[3,4]. Phase III studies have also been conducted to assess the efficacy and toxicity of concurrent chemoradiotherapy in comparison with that of sequential chemoradiotherapy. In two studies, i.e., a Japanese report[5] and the RTOG9410[6] which employed older, second generation regimens, the survival period was reported to be significantly prolonged by concurrent chemoradiotherapy, although the toxicity was worse. Thus, the standard of treatment for stage III locally advanced lung cancer is currently recognized as concurrent chemoradiotherapy.

During the last decade, the usefulness of several new agents, such as paclitaxel, gemcitabine, vinorelbine and docetaxel, have been studied, usually administered in combination with the platinum compounds. These newer-

agent/platinum combinations, the so-called third generation regimen have been proven to be more effective than second generation regimens, as demonstrated by the increased survival of patients with metastatic NSCLC treated by these regimens.[7-9)]

Since the chemotherapy regimens used in the above-described two reports were second generation regimens, the benefit of introduction of third generation regimens for chemoradiotherapy has begun to be assessed. Although concurrent administration of full-dose chemotherapy and thoracic radiotherapy has been reported to be possible by some investigators, it is considered difficult for many regimens[10,11)], third generation agents can hardly be used at their full doses for concurrent chemoradiotherapy because of the high incidence of toxicity associated with these agents. Therefore, for concurrent chemotherapy with TRT, these chemotherapeutic agents have been used at reduced doses in several reported clinical studies[12,13,14)]. However, some reports have suggested that the marked efficacy of concurrent chemoradiotherapy using third generation chemotherapeutic agents can hardly be achieved using these agents at reduced doses[15)].

However, it remains to be clearly established as to which would

be superior in terms of both the efficacy and toxicity: concurrent chemoradiotherapy using the second generation regimens at full doses, or the third generation regimens at reduced doses. We, the West Japan Oncology Group (WJOG), therefore, performed a phase III study to compare these therapeutic strategies. The doses of the chemotherapeutic agents were determined based on the results of Japanese phase I studies.[16,17)]